To link to this article: DOI: 10.1115/1.4003713
URL: http://dx.doi.org/10.1115/1.4003713

To cite this version: Binder, Nicolas and Le Guyader, Sebastien and Carbonneau, Xavier *Analysis of the Variable Geometry Effect in Radial Turbines*. (2012) Journal of Turbomachinery, vol. 134 (n° 4). pp. 041017.1-041017.9. ISSN 0889-504X

Analysis of the Variable Geometry Effect in Radial Turbines

Nicolas Binder[1]
e-mail: nicolas.binder@isae.fr

Sebastien Le Guyader
e-mail: sebastien.leguyader@isae.fr

Xavier Carbonneau
e-mail: xavier.carbonneau@isae.fr

Institut Supérieur
de l'Aéronautique
et de l'Espace (ISAE),
Université de Toulouse,
10 Avenue Edouard Belin,
BP 54032,
31055 Toulouse Cedex 4, France

The influence of variable geometry stators on the stage behavior is analyzed from both theoretical and experimental points of view. A theoretical analysis of the trajectory of some pressure-ratio lines in a loading-to-flow-coefficient diagram leads to the definition of a specific dimensionless parameter: the reduced section. This parameter is representative of the stator geometric configuration and is thus expected to be a good candidate to describe the variable geometry problem. From a theoretical point of view, this parameter is no less than the formal expression of the link between the geometric configuration of the stator and the behavior of the stage. An experimental approach decomposed in three phases is then led to evaluate this assessment. The results clearly demonstrate the crucial influence of the reduced section in the operating point definition. It leads to the conclusion that from a theoretical point of view, the two solutions mainly used in the industry for variable geometry stages (variation of the height or of the opening position of the stator blades) are equivalent provided that they are sanitized of their respective technological drawbacks. It has also been shown that the geometric configuration of the stator chosen to reach a specific value of the reduced section has some incidence on the efficiency of the stage. This observation gives some opportunities for optimization, for which some axis of reflection is given. [DOI: 10.1115/1.4003713]

1 Introduction

Basically, the only purpose of a turbine stage is to supply energy to devices such as electric generators or compressor stages. This energy is taken from the total enthalpy of the inlet fluid, which varies with the flow conditions and with the application considered. The stage design is focused on this set of information, thus defining the stage specification. Designing is a subtle process requiring as much empiric experience as theoretical knowledge. The development gets even more complex if the stage is meant to run under severe variations of functioning conditions. In this case, the specification (design point) is no more unique. The performance objective might be redefined. For example, an average efficiency level over a wide range of functioning can be preferred to excellent peak efficiency over a limited operating range. In the design process of a radial turbine, it usually leads to consider the necessity of a stator, as it is generally admitted that a vaned stator improves the peak efficiency since it tightens the operating range. An analysis over a large number of stages [1] confirms this assessment. Anyway, a discussion of this conclusion is proposed in Ref. [2], as the configurations (roughness and specific speeds) of vaneless stages were generally not suitable to good efficiency. A strict comparison is then proposed whose conclusions tend to disagree with the general assumption.

Prior to efficiency optimization, the designer should be concerned by the basic ability of a single stage to reach given points in the map. Even with the benefit of the diameter reduction term in the Euler equation, which increases the influence of rotational speed, the characteristic evolution of the mass-flow of a radial turbine is not much wider than that of a simple nozzle (as presented, for example, in Ref. [3]). The operating range of the stage is thus restricted to this characteristic zone of the map: The rest of the map is not accessible. This exclusion of possible operating point can be a problem in some applications. For example, in the case of turbocharging, it limits the good matching between the turbine stage and the engine on its whole operating range. Variable geometry stages have been developed for that purpose. By modifying the stage permeability through the variation of a geometric section in the static part, the reduced mass-flow and the pressure-ratio values are partially discoupled. Different technical solutions exist, focusing on the casing modification (see Ref. [4], for instance) or on the alteration of the vaned stator properties. In the latter, the principle is to adapt the stator throat section to inlet flow conditions, as presented in Ref. [5]. This variation is generally obtained by (i) the modification of the incidence of the stator blades and (ii) the variation of the height of the vanes by using a sliding shroud. On the one hand, the choice of a variable-opening stator raises the necessity of mechanical clearances between the stator blades and the casing where severe secondary flows develop. A quick estimation of the losses generated is accessible in Ref. [6] and, more accurately, in Ref. [7]. Moreover, the clearance is often created by intrusive spacers whose wakes interact with the blades, as presented in Ref. [8] or Ref. [9]. On the other hand, the movable-wall solution imposes partial admission on the height of the rotor with severe secondary flow at the leading edge of the blades. The first solution presents better efficiency levels, according to Ref. [10], due to better inlet incidence adaptation along the operating range.

Beside the discussion over the benefits and drawbacks of each of these technical solutions, it is the variable geometry nozzle concept in itself that should be studied. No clear detail of the physical process is found in the literature. Sporadic design rules are proposed, and few corrections of models were implemented. When found, it is done by considering a variable geometry stage as a derivation of a fixed geometry stage. The adjunction of variable geometry is just treated as another design step, and not as a specificity of the stage, which should lead to a specific design from the beginning. Some attempts were made (Ref. [11], for instance) but lack hindsight in the global variable geometry approach. The present work aims at the global comprehension of the variable geometry effect, whatever the technical solution, and at the identification of the relevant parameters of the problem. In a

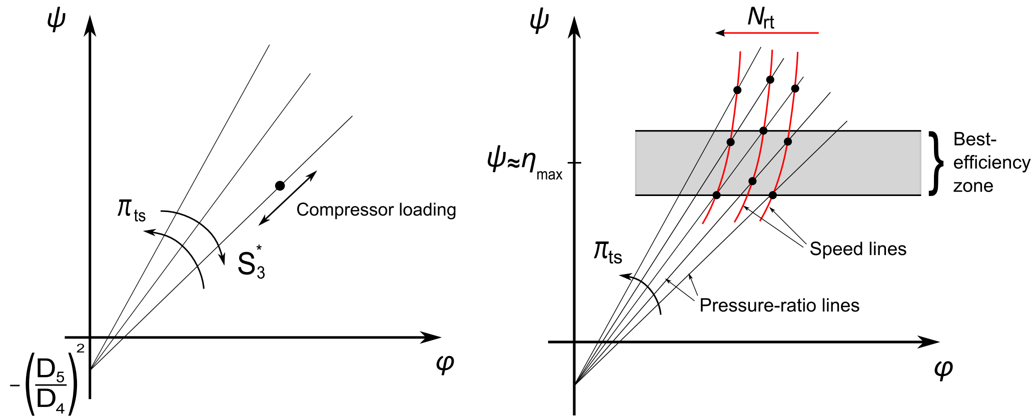

Fig. 1 Pressure-ratio line evolution in a $\psi-\phi$ map

first part, an original theory will be recalled and applied to the variable geometry concept. This theoretical consideration is the basis on which the experimental approach is built and presented in a second part. In the third part of the paper, results are presented and then discussed in a conclusion.

2 Theoretical Issues

From a theoretical point of view, four dimensionless parameters are required to describe the behavior of a radial turbine stage (when neglecting the Reynolds number influence and the gas properties' variations). Usually, those parameters are the reduced mass-flow, the reduced speed, the pressure-ratio, and the efficiency. However, other dimensionless parameters could be used such as flow and loading coefficients defined as follows:

$$\phi = \frac{\dot{m}}{\rho_{i4} U_4 \pi \frac{D_4^2}{4}} \tag{1}$$

$$\psi = \frac{\Delta H}{U_4^2} \tag{2}$$

Recent work [12] has demonstrated the relevance of these parameters by expressing a formal link between them:

$$\psi = \phi \cdot \frac{\pi}{4} \Bigg\{ (\xi \,.\, \pi_{ts})^{1/\gamma} (S_3^*)^{-1} + \left(\frac{P_{i5}}{P_5}\right)^{1-\gamma/\gamma} \frac{D_5}{D_4} (S_5^*)^{-1} \pi_{ts} \left[1 - \eta_{ts} \left[1 - \left(\frac{1}{\pi_{ts}}\right)^{\gamma-1/\gamma} \right] \right] \Bigg\} - \left(\frac{D_5}{D_4}\right)^2 \tag{3}$$

where

$$S_3^* = \frac{S_3}{D_4^2 \frac{D_3}{D_4} \sin(\alpha_3)} \tag{4}$$

$$S_5^* = \frac{S_5}{D_4^2 \tan(\beta_5)} \tag{5}$$

and

$$\xi = \frac{P_5}{P_4} \tag{6}$$

This equation represents the trajectory of a functioning line in a $\psi-\phi$ map. It has thus been shown that for pressure-ratio lines (π_{ts}=const) of a given stage, the trajectory is linear (in that case, Eq. (3) reduces to $\psi = A\phi - B$) with a slope A mainly depending on the pressure-ratio value itself and on two dimensionless cross sections representative of the stator geometry at the throat (S_3^*) and of the rotor geometry at the outlet (S_5^*). The intercept B is defined by the trim of the rotor. Figure 1 illustrates this theoretical result and the features of this alternative turbine map describing the stage behavior.

This assessment gives a new perspective to the variable geometry concept. Generally, the variable geometry effect is associated with a variation of a geometric section of the stator. Actually, the behavior alteration is more likely to originate from a variation of the reduced section. For a given pressure-ratio, shifting the stator geometry changes the value of S_3^*. Subsequently, the slope of the pressure-ratio line is modified: The functioning trajectory has changed.

This property of pressure-ratio lines has been observed in both experimental (see Ref. [12]) and numerical (see Ref. [13]) results with quite good agreement. However, reality differs slightly from the theory concerning the intercept of the lines. According to Eq. (3), the intercept is constant and common to each of the lines. A displacement of this point has been observed and correlated with the evolution of the intermediate pressure-ratio ξ. Anyway, S_3^* seems to be a good candidate as a parameter to describe the variable geometry problem. Its presumed importance in the process is at the very core of this experimental study, the approach of which we will now describe.

3 Experimental Approach

The theoretical analysis leads to consider that the value of S_3^* is most important in the variable geometry process. In that line, three statements follow.

1. If the reduced section variation is the dominant effect, then both of the classical solutions (opening or blade's height variation) are equivalent provided that they are sanitized of their technological drawbacks (spacers, stator clearances, partial loading at the inlet of the rotor, etc.).
2. It should be possible to reproduce the behavior of a variable-opening stator without changing the opening angle.
3. Two different geometric stator configurations generating the same value of reduced section should behave the same way.

In order to examine these assessments, series of stator geometries are tested on a reference stage.

3.1 Geometric Configurations of the Stator. The definition of S_3^* in Eq. (4) expresses an implied dependence to geometric factor constituting the stator. More specifically, for a given blade section, the value of S_3^* can be modified by changing (see Fig. 2 for illustration) the following:

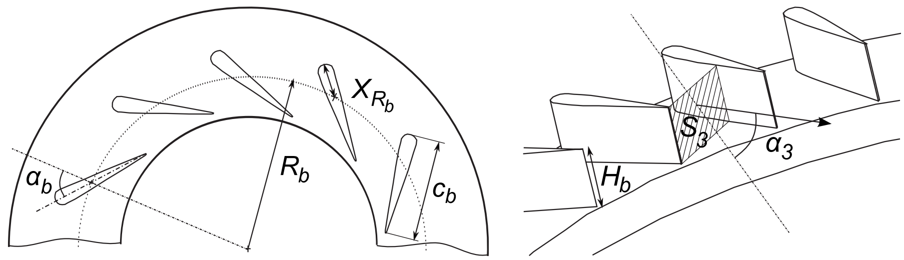

Fig. 2 Geometric factors of the stator

- the angle of the blades (α_b)
- the height of the blades (H_b)
- the radial position of the blades (R_b)
- the chord of the blades (c_b)
- the number of blades (N_b)

It has been decided that the reference on the blade to set the radial position R_b should be a fixed position from the leading edge. This particular point (X_{R_b}) is thus at a fixed distance from the leading edge, whatever the actual chord of the blade. It is also the point for which the blade's angle α_b is measured. This point would be the position of the pivot on a classic variable-opening stator.

The dependence of the reduced section to these parameters cannot be expressed by an analytic expression. A specific routine, taking the airfoil section into account, has been developed to obtain the value of the geometric cross section (S_3) at the throat of the stator. The characteristic radii and angles are also estimated in order to build the reduced section of a known stator geometry as accurately as possible. However, a given value of S_3^* can be obtained by different combinations of the geometric factors.

Three groups of stator configurations are defined according to the three aforementioned statements. The first deals with the comparison between the two variable geometry solutions (height or opening variation). This group is a series of declinations of the reference stator, by variation of the opening angle (five values of α_b from closed to open position), and of the blade's height (three values of H_b). Fifteen stator configurations are thus implemented on the stage without clearances at the hub and shroud. In order to avoid partial loading at the inlet of the rotor, it has been decided to match the rotor inlet to the stator blade's height, even if it implies a modification of the rotor geometry. The trimming configuration of the inducer of the rotor is thus adapted to the modifications of the height of the stator blades; the rotor outlet diameter is identical for all of the geometries. At initial blade's height, the stators are quoted from 1 (closed position) to 5 (open position). Stator 3 is the reference stator. Then, "small" stators $1s$–$5s$ (small height of blades) are defined together with the "high" stators $1h$–$5h$ (high height of blades). The characteristics of the stators are given in Table 1.

The second group of stators aims at the segregation of the influences of the reduced section and the opening position. In that purpose, four stators were built with the opening angle of the blades fixed at the reference opening position. Modifications of the other parameters are then applied in order to match the reduced section value of the successive opening position of the initial geometries. These configurations are the "modified" configurations: $1m$, $2m$, $4m$, and $5m$ whose characteristics are recalled in Table 2. For example, configuration $1m$ has the same reduced section value as configuration 1 for the same opening angle of the blades as the reference configuration (stator 3).

The last group is a set of four different configurations having the same reduced section value as the reference stator, still for the reference opening angle. The extensive variation of opening angle at the fixed reduced section is a forthcoming step of the study, which has not been conducted yet. Those stators are thus declinations of stator 3: $3a$, $3b$, $3c$, and $3d$. The characteristics are also given in Table 2.

In the two latter groups, one can note that some configurations are rather "exotic." Both $5m$ and $3a$ propose a very small number of blades with/or a small chord. An illustration of these configurations is proposed in Fig. 3. A bad guiding of the flow can be there expected. Despite the fact that setting the geometric parameters to match a given reduced section is not an easy process and does not propose an infinity of possibilities due to construction constraints, those combinations could have been avoided. But, the response of such unreasonable configurations seems interesting to gauge the limitations of the reduced section influence.

The values given in Tables 1 and 2 are the theoretical ones in order to clarify the approach (quoted S_3^* in the tables). A metrologic verification of the geometries has been conducted after the physical construction of the different stators. A difference in terms of the reduced section has been observed, but in small proportion as the mean deviation between theoretical and real values is around 6% (the values obtained are presented in the tables as $S^*_{3_{\mathrm{metro}}}$). All the results and correlations presented in the forthcoming section of course display the real values of the reduced section given by metrology.

3.2 Experimental Device. The test was conducted on our "Petite TurboMachine" (PTM) test rig dedicated to turbocharger application. This steady flow test rig allows either global or local instrumentation of small stages for a wide range of inlet temperatures (from 20°C to 620°C) up to 250 g/s. The air is supplied by a pressure source (6 bars) stabilized by two regulation stages. The compressor and turbine flows are independent. They are thermally isolated from the ambient air and from one another. A specific circuit supplies hot and pressurized oil to the bearings. Inlet and outlet pressures and temperature are acquired in order to measure the performance of both of the stages. Mass-flow measurement is operated through a Coriolis flowmeter. Rotational speed is counted using a proximity sensor on the compressor stage. For

Table 1 Characteristics of the first group of stators

Stator	$\Delta\alpha_b$ (deg)	$\frac{H_b}{H_{b_{\mathrm{ref}}}}$	S_3^*
1	−15	1	**0.074**
2	−10	1	**0.116**
3(ref)	0	1	**0.215**
4	+10	1	**0.330**
5	+22	1	**0.520**
…	…	…	…
$2s$	−10	**0.71**	0.086
$3s$	0	**0.71**	0.154
…	…	…	…
$4h$	+10	**1.13**	0.378
$5h$	+22	**1.13**	0.596

Table 2 Characteristics of the second and third groups of stators

Stator	$\Delta\alpha_b$ (deg)	$\frac{H}{H_{\text{ref}}}$	N_b	$\frac{c_b}{c_{b_{\text{ref}}}}$	$\frac{R_b}{R_{b_{\text{ref}}}}$	S_3^*	$S^*_{3_{\text{metro}}}$
1*m*	0	0.70	ref+6	1.34	0.93	**0.074**	0.072
2*m*	0	0.70	ref+1	1.03	0.94	**0.116**	0.117
4*m*	0	1.13	ref–3	0.97	1.13	**0.330**	0.350
5*m*	0	0.89	**ref–7**	0.97	1.11	**0.520**	0.516
3*a*	0	0.75	**ref–2**	**0.62**	0.89	**0.215**	0.247
3*b*	0	1.13	ref	1.01	0.89	**0.215**	0.228
3*c*	0	0.70	ref–5	1	0.96	**0.215**	0.235
3*d*	0	0.86	ref+5	0.57	0.96	**0.215**	0.216

more details about the test facility, see Ref. [14]. As the experimental study deals with comparative results, it is the repeatability quality of the experimental device that mainly imports. The confidence ranges are given in Table 3 for the nondimensional quantities mostly considered in the results.

For machining convenance, the prototype stators were built with aluminum alloy (AU4G), which does not sustain high temperatures. The test was then conducted under ambient temperature for the air flow supplied to the turbine stage. The pressure-ratio lines are described for different values (π_{ts} from 1.4 to 1.9) by modifying the loading of the compressor controlled by a discharge valve. A minimum of four points per line is acquired. For the reference configuration, the range of the pressure-ratio lines is widened by using compressor impellers of different diameters. The results obtained are now presented.

4 Results

The presentation of the post-treated results is now proposed in three sections according to the three axes identified for the approach. The numerical results for the reduced mass-flow, reduced speed, and efficiency are given as fraction of the values of a reference operating point. This point is located on the pressure-ratio line $\pi_{\text{ts}}=1.8$ for the reference stator (stator 3).

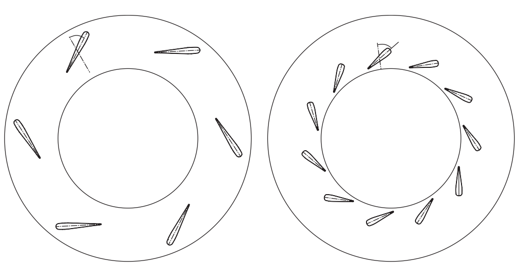

Fig. 3 Geometries for which a bad guiding of the flow is expected

Table 3 Repeatability uncertainty of the bench

Quantity	95% confidence range (%)
Q_{rt}	± 0.3
N_{rt}	± 0.2
π_{ts}	± 0.15
η	± 1
ϕ	± 0.3
ψ	± 1.2

4.1 Relative Influence of Stator Height and Opening Position.

Figure 4 presents the evolution of the pressure-ratio lines obtained with the different stators in the $\psi-\phi$ map. First, the opening angle is the only parameter modified, the height being fixed at the reference value (Fig. 4). Second, both of these parameters are altered (Fig. 5). In Fig. 4, the linearity of the pressure-ratio lines is remarkable. This observation strongly supports the theoretical development proposed above. Beside this observation, the influence of the opening position via the reduced section (S_3^*) on the slope of the lines is confirmed. Now, in Fig. 5, the same mechanism can be observed for a given opening position when changing the stator height: The stator height modification induces an alteration of the value of the reduced section, thus changing the slope of the lines. As fewer points were taken in that configuration due to the small operating range allowed by the compressor, this assessment is not strongly perceptible on the figure. The values of the slope A are thus plotted against the reduced section of the successive stators for a fixed pressure-ratio ($\pi_{\text{ts}}=1.8$) in Fig. 6. A regular decrease is observed. This decrease of A is compared with a theoretical variation (from Eq. (3), we expect that $A \propto (S_3^*)^{-1}$) with quite good agreement.

Eventually, the functioning trajectory in the $\psi-\phi$ map strongly depends on the value of the reduced section, whatever is the origin of its variation (stator opening position or blade's height alteration), as was predicted by the theory. To illustrate this equivalence, Fig. 7 gives a classic representation of the turbine map. For both the small- and the large-height configurations of the blades, the results of the five opening configurations of the stators have

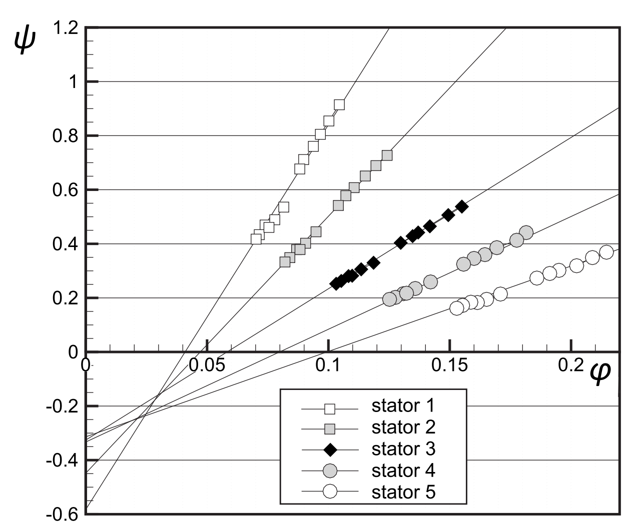

Fig. 4 $\psi-\phi$ map at $\pi_{\text{ts}}=1.8$ for all the opening positions of the reference stator

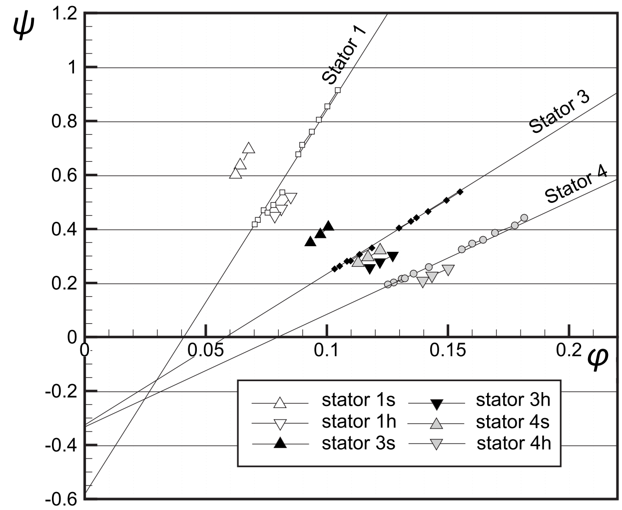

Fig. 5 $\psi-\phi$ map at $\pi_{ts}=1.8$ for some combined variations of stator opening position and stator height

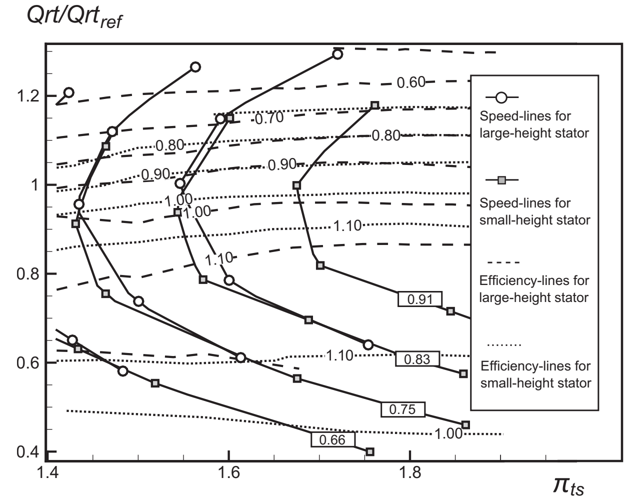

Fig. 7 Superposition of the map for both high and small stator heights. Numerical values are relative to the reference state.

been interpolated to identify the speed-lines and the efficiency-lines for a given compressor loading configuration. This artificially defines two variable-opening stages with different stator heights. The two maps then built are superposed in Fig. 7; the numerical values are given as fraction of the reference operating point. These two maps here present the characteristic features of a variable geometry stage map: a large range of reduced mass-flow for given pressure-ratio and incurved speed-lines reaching a minimum pressure-ratio value near the maximum efficiency zone. The two stages do not cover the same regions in the map, but an overlapping zone is observed at the center of the chart. In that zone, a strong correspondence of the two sets of curves is perceptible. Either the speed-lines or the efficiency-lines are almost superimposed from one stage to another, and the isovalue is the same. From this zone, the large-height stage extends to the largest mass-flow values, and the small-height stage to the lesser ones, just as if the two stages were in continuity from one to another. The fraction of this extended map covered by a stage is given by the range of the reduced section that the geometry is able to produce. Obviously, when the reduced section is no more variable, the zone is almost restricted to a single line: It reduces to a classic fixed geometry turbine map.

Figure 8 illustrates the importance of the reduced section value in the identification of the overlapping zone between the stages. With S_3^* and π_{ts} fixed, and for a given loading of the compressor, the mass-flow and the rotational speed are identical for the three stages, even if the physical value of opening angle or height is different. An overlapping region is found in the map if the reduced section ranges of the three stages overlap also.

This assessment leads to the conclusion that the two solutions (opening or height variation) are equivalent provided that the technological effects are discarded, which is not the case in reality. Basically, the choice to adopt one of the two solutions should be considered through the actual ability to limit the losses associated with one or the other. But, in principle, they are of equivalent validity. The key to the problem is the variation of the reduced section. If the right variation is ensured, the right operating range seems almost guaranteed even if some dispersion in the performance is observed (efficiency-lines are not strictly superimposed in Fig. 7).

Stator opening and height are not the only physical possibilities to interfere with the reduced section value. As explained in the first part of the paper, three more geometric parameters are in-

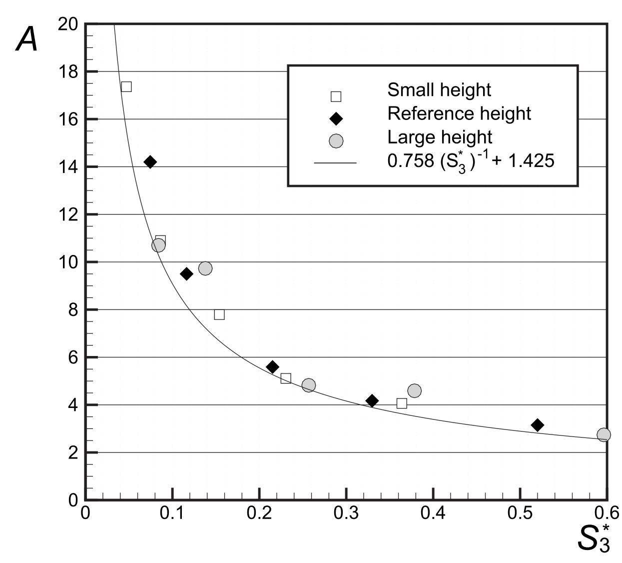

Fig. 6 Variation of the pressure-ratio line's slope with the value of S_3^*

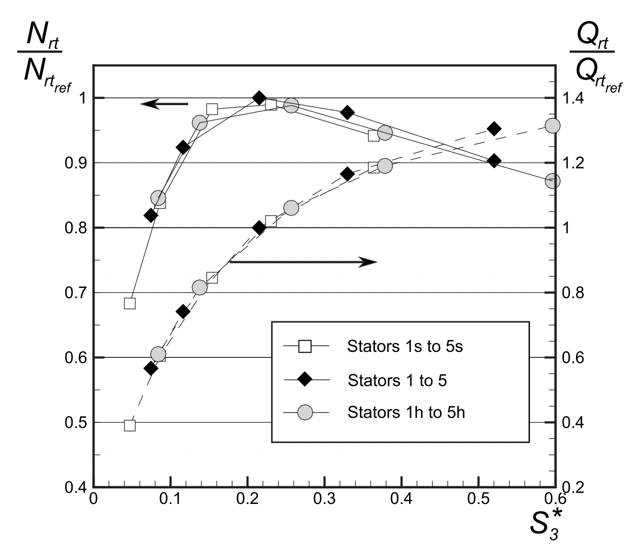

Fig. 8 Mass-flow and rotational speed evolution against the reduced section for $\pi_{ts}=1.8$

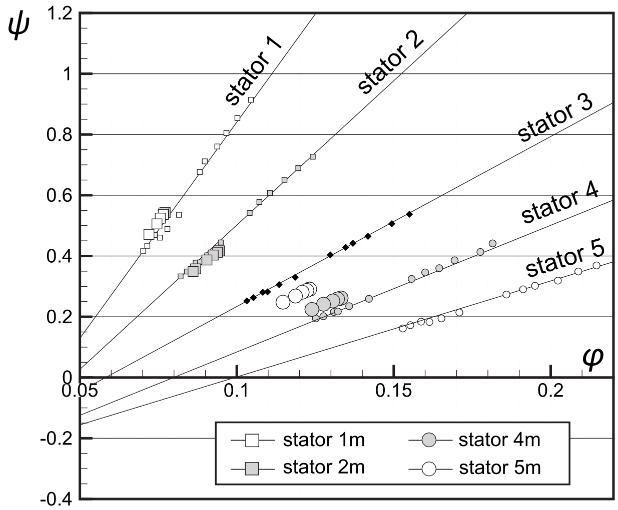

Fig. 9 Equivalence in the $\psi-\phi$ map of initial and modified configurations for $\pi_{ts}=1.8$

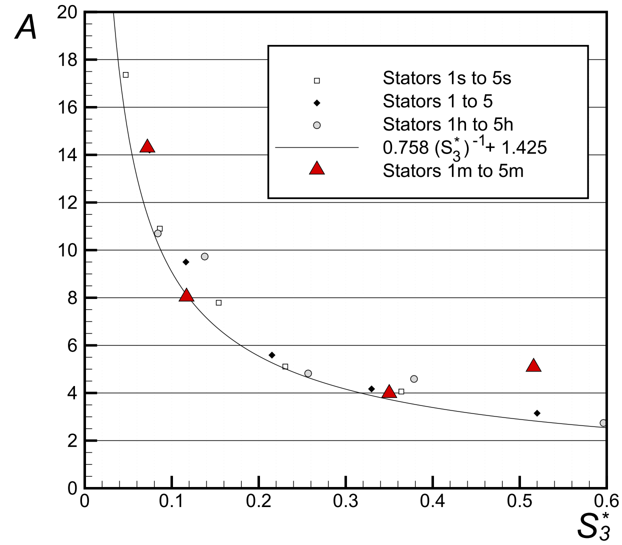

Fig. 10 Pressure-ratio line's slope of the modified configurations

volved in the definition of S_3^*. Thus, there might be, for a given reduced section, an optimal geometric construction. The second step of the approach then brings the other geometric parameters of the stator into the study to confirm the importance of the reduced section and have a first discussion about performance.

4.2 Generalization to Other Parameters. Here, the results of stators $1m, \ldots, 5m$ are presented. This succession of configurations aims at reproducing the behavior of a variable-opening stator without changing opening configuration. All the other parameters (H_b, c_b, N_b, and R_b) are thus modified to perform the geometry variation. On the $\psi-\phi$ map of Fig. 9 are plotted the four pressure-ratio lines of the modified configurations compared with the five reference configurations. The linearity is still verified compared with the reference machine even if fewer points were acquired. Configurations $1m$, $2m$, and $4m$ are very close to their related initial configuration: The experimental points are almost located on the linear regression obtained for the initial geometry of the stators despite the fact that the opening angle is different. However, configuration $5m$ is quite different from its original declination. It seems closer to stator 3 rather than stator 5. This kind of result was expected from the very beginning of the study, as we have already pointed out that configuration $5m$ does not give a proper definition of the interblade channels due to its low number of small blades (as was illustrated in Fig. 3). As a result, it is quite difficult to identify a throat and thus an adequate definition of the reduced section. Here, the fact that the result is quite similar to stator 3 better than stator 5 suggests that some phenomenology, most likely separations, reduces the actual geometric value of the reduced section to a lesser effective one. However, without local data, this assumption is purely conjectural. Some computational fluid dynamics (CFD) could be most useful in that purpose and is scheduled in forthcoming work.

The slope values of the lines obtained with configurations $1m, \ldots, 5m$ are plotted in the correlation between slope and reduced section value (see Fig. 10). Here, the modified configurations merge completely in the trend of what was defined by the variable-opening configurations. It reinforces the predominance of the reduced section value over any geometric factor to define the pressure-ratio line in the $\psi-\phi$ map. Quite logically, configuration $5m$ is not in the normal evolution and presents a slope higher than what could be expected for reasons explained above.

The results obtained are also compared with what was presented in Fig. 8. In Fig. 11, a best fit evolution has been defined using all the configurations of the first step of the study $(1s, 2s, \ldots, 3, \ldots, 5h)$; the reference stators' value has been explicitly transferred. Here, the pressure-ratio is fixed ($\pi_{ts}=1.8$) together with the compressor loading configuration. The modified configuration results are thus compared with this expected evolution. The result speaks for itself either for rotational speed or for the reduced mass-flow. Except for configuration $5m$, the modified stators describe accurately the expected evolution. In other words, whatever the geometric factor choice to perform geometry variation, as long as the reduced section value is kept constant, the stage behavior is not strongly affected. However, the question of efficiency is raised. Figure 12 presents the evolution of the total-to-static isentropic efficiency against mass-flow for the reference and the modified configurations at the fixed pressure-ratio. The configurations presented on the first part of the paper were also plotted. Once again, the modified configuration follows the expected trend. The typical deviation compared with the reference configuration is completely in the range of what was observed when changing the stator blades and height. It confirms the fact that the choice of the geometric parameter operating the geometry variation is not such an important choice from a theoretical point of view. It is the value of the reduced section that defines the

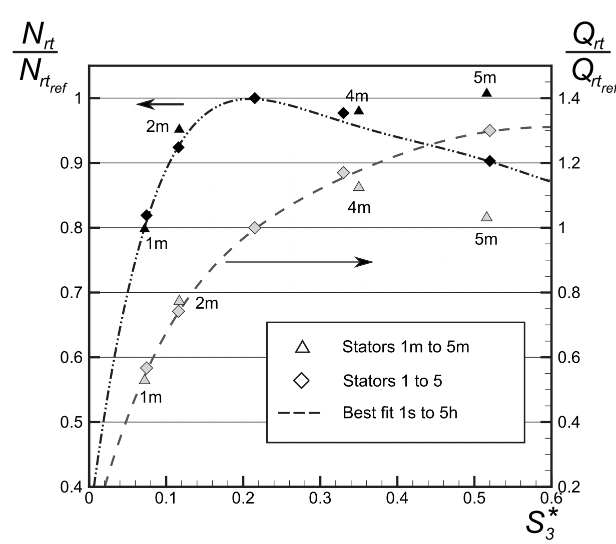

Fig. 11 Reproduction of the variable geometry behavior without opening-configuration modification

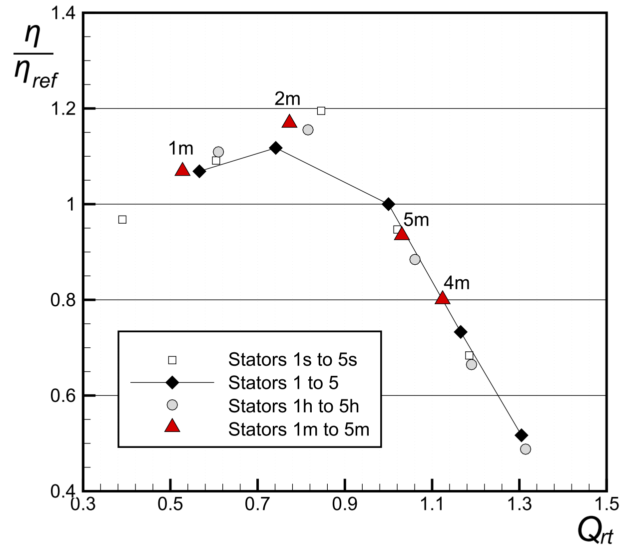

Fig. 12 Efficiency evolution with the mass-flow for $\pi_{ts}=1.8$

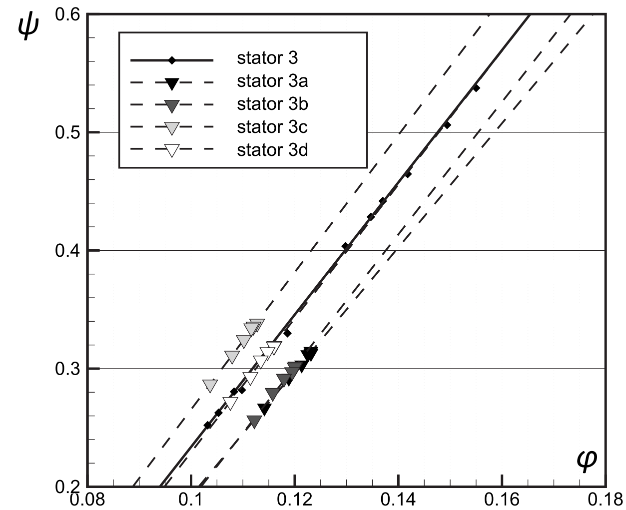

Fig. 13 $\psi-\phi$ map at $\pi_{ts}=1.8$ for the different geometries having the same reduced section value ($3a,\ldots,3d$)

operating point and an order of magnitude for the performance for a given pressure-ratio and a given loading configuration of the compressor. However, we can observe that some configurations give better results than others. For example, stator $2m$ proves more efficient than the reference geometry. This means that besides the obtention of a given operating point, some latitude for improvement is available. Surprisingly, configuration $5m$ is definitely integrated to the evolution, but not at the expected location: The results are very similar to those of a lower reduced section configuration, which once again points out that some blockage must occur.

We have then proved that the value of the reduced section defines the operating point for a given pressure-ratio. This is true provided that the stator has a "reasonable" construction (i.e., a good guidance of the flow is supplied by the stator blades). However, quite logically, some variations in the performance for given S_3^* have been observed. It leads to focus on the influence of the geometric construction on the efficiency of a given reduced section. This analysis is now performed.

4.3 Importance of Geometric Construction. Even if the reduced section defines the operating point, we have shown above that it does not constrain efficiency. For a given value of S_3^*, different geometric configurations are possible to design, but are not equivalent in terms of performance. This dependence of the efficiency to the geometric construction is due in part to the complex local process of rotor/stator interaction, difficult to apprehend and beyond the scope of this paper. However, some observations can be made. The stators $3a,\ldots,3d$ have been designed in order to present the same value of S_3^* as the reference configuration. The same stage behavior is then expected from all of these configurations. In Fig. 13 are presented the results of the stators in the $\psi-\phi$ map compared with the reference stator at $\pi_{ts}=1.8$. The evolution is still linear for each of the configurations. The slope of the line is quite the same as the different lines are almost perfectly parallel to the reference stator line. However, an offset is observed between the evolutions.

The stage behavior is presented by using the usual indicators in Fig. 14. The variations of reduced mass-flow and rotational speed against the pressure-ratio display a deviation between the different configurations. It is very small regarding the rotational speed (less than 2%), but the mass-flow differs by $\pm 5\%$ compared with the reference configuration. Here, the metrologic control of the geometries has proved useful, as it revealed the fact that the actual reduced section of configuration $3a$ was slightly greater than the reference configuration, as was presented in Table 2. The difference of geometry should explain most of the deviation. But, the possibility of interference of the geometric construction on some local phenomenology exists. For example, configuration $3c$ is close to the reference stator in terms of the actual value of the reduced section and still presents a deviation in the mass-flow value, which is not fully understood.

However, beside the exact reproduction of the operating point, the evolution of efficiency is most interesting. In Fig. 15 is presented the evolution of the efficiency against the reduced tip-speed for the four declinations of the reference stator compared with the reference geometry (a polynomial interpolation has been operated for the reference stator). Two pressure-ratio lines are considered ($\pi_{ts}=1.4$ and 1.8) for each configuration. Two main observations are retained: First, the two pressure- ratio lines are almost in continuity from one to another in this diagram, whatever the configuration considered. This is the expression of the important correlation between reduced tip-speed and efficiency for radial turbine stages. This has been widely presented and explained in the literature with the well known optimum found around $U/C_s=0.7$. In fact, a lot of prediction process makes the assumption of the unicity of this evolution for a given stage in order to

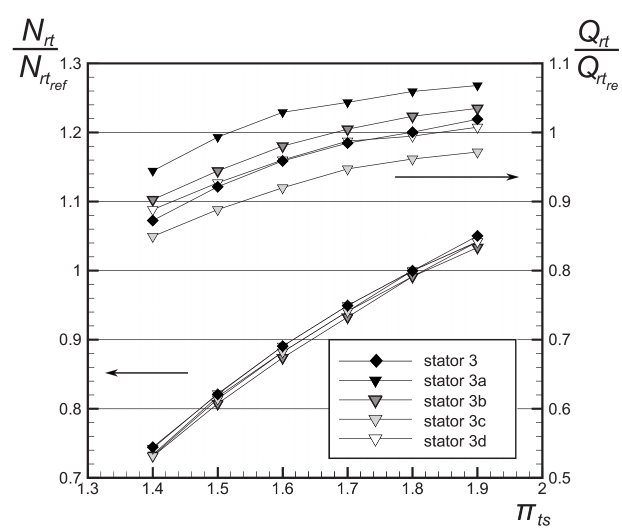

Fig. 14 Mass-flow and rotational speed evolutions against the pressure-ratio value

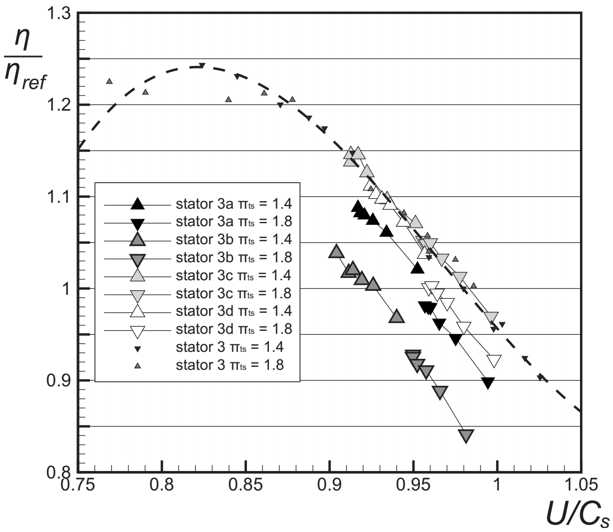

Fig. 15 Efficiency evolution against the reduced tip-speed

obtain the order of magnitude of efficiency. The second observation is the clear hierarchy between the configurations. Configuration $3c$ is a match for the reference configuration and configuration $3b$ clearly presents the worst performance. The explanation of this difference cannot be simple since it is an expression of the complex physical phenomenon occurring between the rotor and the stator. Choosing a global indicator expressing local behavior in order to classify the configurations is thus challenging. One choice is the free space parameter found in Ref. [15] whose expression is recalled in Eq. (7),

$$\Delta R^* = \frac{R_3 - R_4}{H\cos(\alpha_3)} \tag{7}$$

This indicator is a nondimensional expression of a trajectory estimation of the particles in the free space between the stator and the rotor. An optimum was observed and reputed to be found around $\Delta R^*=2$. It is obvious that this criterion will not allow to take into account the full complexity of the loss process occurring in the real flow, but has the advantage to be built with data available at the very beginning of the design process. A correlation between the performance of the different configurations and the free space parameter is proposed in Fig. 16. A global trend is observed,

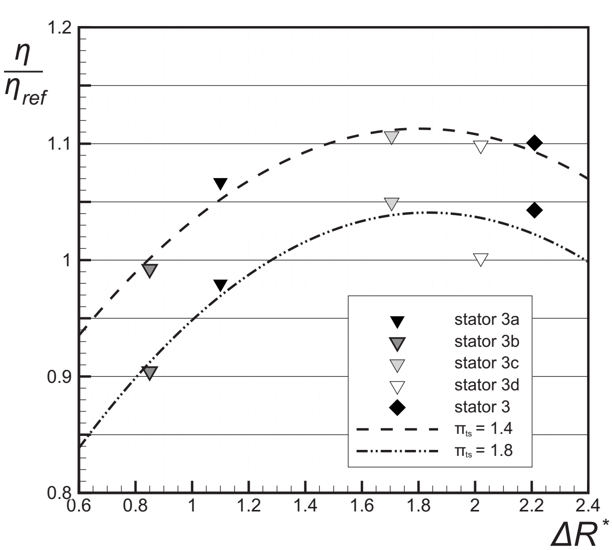

Fig. 16 Efficiency evolution against the free space parameter

reaching an optimum almost centered on 2, for two different values of the pressure-ratio. But, the fact that few geometries were tested and the range of ΔR^* being restrictive does not allow to be strictly conclusive about the relevance of the parameter. More specifically, one can note the deviation of configuration $3d$ from the trend, which appends to be the configuration having the most important number of blades. It thus leads to consider the necessity of other criteria describing the performance potential of a given geometry, as it is needed in the classic stator design. But, it must be reminded that in the variable geometry context, some choices appearing good for a given position of the nozzle can prove disastrous for another one. Finally, the choice of the design nozzle-position has as much importance as the design itself.

5 Conclusion

Both theoretical and experimental analyses have been conducted in order to understand the variable geometry process in radial turbines. The use of an alternative to the usual turbine map eases the understanding of such an effect, highlighting the nondimensional section of the stator as a key parameter to the problem. Based on the presumed importance of this reduced section in the variable geometry process, a specific approach involving the extensive variation of parameters of the geometry has been built, and tests were conducted. The results allowed discussing the statements expressed at the beginning of the paper. Summarizing, we have shown the following.

1. From a theoretical point of view, yes, both the solutions found in the industry for variable geometry stages (variable opening or variable height) are equivalent, but are not in reality because some technological drawbacks are unavoidable.
2. Yes, it is possible to reproduce the exact behavior of a variable-opening stator without changing the stator opening angle.
3. Two configurations with different geometric configurations but with the same value of reduced section tend to behave the same way.

Some divergence from the expected behavior, predicted by the theory, was observed. Some of those divergence were due to a perfectible conformity of the geometry built, but other were inherent to the stage functioning. This was expectable as the complex tridimensional flow occurring in the stage cannot be completely modeled by a one-dimensional approach. Even if they proved of a small order of magnitude, those divergence need more local data in the stator region to deepen the analysis. But, small divergence can have dramatic consequences on the efficiency of a stage. In that field, we presented the free space criterion as a good candidate to apprehend the performance potential of a geometry for a given reduced section value. Other criteria exist and should be gathered from the literature focused on the design process of the stator. In the author's view, the right combination of them is probably necessary to propose adequate correlations. A judicious parametric study at constant reduced section could also precise these correlations since the geometric factors constituting the stator should be classified in importance. Anyway, some part of the operating range of a variable geometry stage can be favored compared to other ones, since it might not be possible to match the proper design criteria for all of the stator positions. This should be taken into account in the very first steps of the design process, and not analyzed subsequently.

Nomenclature

Roman

A = gradient of the pressure-ratio lines
C_b = chord of the blades
C_s = isentropic speed

D = diameter
H = enthalpy
$\dot{m}$ = mass flow rate
N_b = number of blades
N_{rt} = nondimensional rotational speed
P = pressure
Q_{rt} = nondimensional mass flow rate
R = radius
S = geometric cross-section area
S^* = reduced cross-section area
U = tip-speed

Greek

α = absolute flow angle
α_b = opening angle of the blades
β = relative flow angle
γ = specific heat ratio
η = efficiency
ξ = intermediate pressure-ratio
π = pressure-ratio
ρ = density
ϕ = flow coefficient
ψ = loading coefficient

Subscripts

3 = stator outlet
4 = rotor inlet
5 = rotor outlet
ts = total-to-static state
ref = reference state

References

[1] Baines, N. C., and Lavy, M., 1990, "Flows in Vaned and Vaneless Stators of Radial Inflow Turbocharger Turbines," IMech Paper No. C405/005.
[2] Spence, S., Rosborough, R., Artt, D., and McCullough, G., 2007, "A Direct Performance Comparison of Vaned and Vaneless Stators for Radial Turbines," ASME J. Turbomach., **129**(1), pp. 53–61.
[3] Lakshminarayana, B., 1996, *Fluid Dynamics and Heat Transfers of Turbomachinery*, Wiley Interscience, New York.
[4] Chappie, P. M., Flynn, P. R., and Mulloy, J., 1980, "Aerodynamic Design of Fixed and Variable Geometry Nozzleless Turbine Casings," ASME J. Eng. Power, **102**(1), pp. 141–147.
[5] Baines, N. C., 2005, *Fundamentals of Turbocharging*, Concepts ETI.
[6] Meitner, P. L., and Glassman, A. J., 1980, "Loss Model for Off-Design Performance Analysis of Radial Turbines With Pivoting-Vane, Variable-Area Stators," SAE Technical Paper No. 801135.10.4271/801135
[7] Qiu, X., Anderson, M. R., and Baines, N. C., 2009, "Meanline Modeling of Radial Inflow Turbine With Variable Area Nozzle," ASME Paper No. GT2009-59170.
[8] Fukaya, M., and Watanabe, A., 2000, "Compressible Turbulent Flow Analysis on Variable Nozzle Vane and Spacers in Turbochargers Turbine," SAE Technical Paper Series 2000-01-0526.
[9] Binder, N., Carbonneau, X., and Chassaing, P., 2004, "Volute Outlet Conditions Study by Measurements on the Stator Blades of a Small Dimension Radial Turbine Stage," Third International Conference on Heat Transfer, Fluid Mechanics and Thermodynamics.
[10] Moustapha, H., Zeleski, M. F., Baines, N., and Japikse, D., 2003, *Axial and Radial Turbines*, Concepts ETI.
[11] Zhang, J., Zhuge, W., Hu, L., and Li, S., 2007, "Design of Turbocharger Variable Nozzle," *Proceedings of the ASME Turbo Expo 2007*, Montreal, QC, Canada.
[12] Binder, N., Carbonneau, X., and Chassaing, P., 2008, "Off-Design Consideration Through the Properties of Some Pressure-Ratio Line of Radial Inflow Turbines," Int. J. Rotating Mach., **2008**, p. 273296.
[13] Carbonneau, X., and Binder, N., 2009, "Analysis of the Pressure-Ratio Lines for Radial Turbines," *Proceedings of the Eighth European Turbomachinery Conference (ETC 8)*.
[14] Binder, N., Carbonneau, X., and Chassaing, P., 2005, "Influence of a Variable Guide Vane Nozzle on the Design Parameters of a Radial Turbine Stage," *Proceedings of the ETC 2005*, Lille, France.
[15] Watanabe, I., Ariga, I., and Mashimo, T., 1971, "Effect of Dimensional Parameters of Impellers on Performance Characteristics of a Radial Inflow Turbine," ASME J. Eng. Power, **93**(1), pp. 81–102.